First identification of collective bands and octupole correlations in the neutron-rich ^{143}La nucleus

J. G. Wang,[1] S. J. Zhu,[1,2,*] J. H. Hamilton,[2] A. V. Ramayya,[2] J. K. Hwang,[2] Y. X. Luo,[2,3] Y. J. Chen,[4] J. O. Rasmussen,[3] I. Y. Lee,[3] X. L. Che,[1] H. B. Ding,[1] K. Li,[2] C. T. Goodin,[2] and Q. Xu[1]

[1]*Department of Physics, Tsinghua University, Beijing 100084, People's Republic of China*

[2]*Department of Physics, Vanderbilt University, Nashville, Tennessee 37235, USA*

[3]*Lawrence Berkeley National Laboratory, Berkeley, California 94720, USA*

[4]*China Institute of Atomic Energy, P.O. Box 275(18), Beijing 102413, People's Republic of China*

(Received 5 March 2007; published 1 June 2007)

The high-spin levels in the neutron-rich ^{143}La nucleus have been investigated from the study of prompt γ rays in the spontaneous fission of ^{252}Cf with the Gammasphere detector array. A new level scheme with spin up to 27/2 $\hbar$ has been established, and the collective bands have been identified for the first time. A set of opposite-parity bands connected by $\Delta I = 1E1$ crossing transitions gives evidence for octupole correlations. The results of $B(E1)/B(E2)$ branching ratios indicate that the octupole correlations in ^{143}La are strong. The reflection-asymmetry shell model is applied to calculate the levels of the octupole bands of ^{143}La, and the calculated results are in good agreement with the experimental ones.

DOI: 10.1103/PhysRevC.75.064301 PACS number(s): 21.10.Re, 23.20.Lv, 27.60.+j, 25.85.Ca

I. INTRODUCTION

A nucleus with octupole deformation has an asymmetric shape in its intrinsic frame. In such nuclei, the level structure has the characteristics of alternating parity bands intertwined by $E1$ transitions. Theoretical calculations in the deformed shell model suggest the existence of an island of octupole-deformed nuclei around $Z = 56$ and $N = 88$ [1–3]. In previous experimental studies, octupole-deformed bands and strong octupole correlations have been observed in many nuclei in this region, especially in $Z = 56$ Ba and $Z = 58$ Ce neutron-rich isotopes, such as, in $^{140-146}$Ba [4–9], and ^{144,146,148}Ce [5,10–12] by measuring the prompt γ rays from the spontaneous fission of actinides. For $Z = 57$ La isotopes, strong octupole correlations also were reported in ^{145,147}La [13,14].

To search for new octupole correlations in this region, it can be expected that the neutron-rich ^{143}La nucleus with $Z = 57$, $N = 86$ is a good candidate, as it lies inside this octupole deformed island. In the previous β-decay experiments [15–17], many low-spin levels have been identified in ^{143}La, but no collective band has been reported. In this work, we report on identification of new collective bands with high-spin states and octupole correlations in ^{143}La.

II. EXPERIMENT AND RESULTS

The high-spin states of ^{143}La in the present work have been investigated by measuring the prompt γ-rays emitted from the fragments produced in the spontaneous fission of ^{252}Cf. The experiment was carried out at the Lawrence Berkeley National Laboratory. A ^{252}Cf source of strength $\sim$60 μCi was sandwiched between two Fe foils of thickness of 10 mg/cm^2. The source then was placed at the center of the Gammasphere detector array [18] which, for this experiment, consisted of 101 Compton-suppressed Ge detectors. A total of 5.7×10^{11} triple- and higher-fold γ-coincidence events were collected. Thus, these data have higher statistics than our earlier measurements of Refs. [8,13] by a factor of about 15. Detailed information of the experiment can be found in Refs. [5,8]. The coincidence data were analyzed with the RADWARE software package [19].

The new level scheme of ^{143}La in the present work is shown in Fig. 1. It was deduced from γ-γ-γ coincidence relationships, transition intensity analysis and total internal conversion coefficient measurements. Two low-excitation levels at 29.9 and 291.5 keV, along with three transitions of 29.9, 261.6, and 291.5 keV in Fig. 1 have been identified in the previous β-decay studies [15–17]. We add 20 new transitions and 13 new levels in the new scheme. As examples, Fig. 2 gives two double gating coincidence γ ray spectra. In Fig. 2(a), the γ ray spectrum is obtained by double gating on the 291.5 and 663.6 keV γ transitions. One can see a strong 498.3 keV γ peak, and all the transitions above the $13/2^+$ level, 690.3 and 655.1 keV in band (1), 595.2, 641.1, and 614.1 keV in band (2), 325.8, 364.5, 230.7, and 424.4 keV between bands (1) and (2), 404.9 keV from band (3) to band (1), and 615.0 keV (overlapped with the 614.1 keV γ peak) in band (3). Figure 2(b) shows a coincidence spectrum with the double gated energies of 291.5 and 498.3 keV. One can see most of the γ transitions above the $9/2^+$ level in Fig. 1. From each spectrum, one can also see the known partner's transitions, such as the 159.3 and 218.5 keV ones in ^{103}Nb ($6n$) [20], and 128.0 (mixed with the 128.0 keV transition in ^{143}La), 162.4 and 220.6 keV transitions in ^{105}Nb ($4n$) [21].

Three new collective bands are observed and are labeled as (1), (2), and (3) on the top of the scheme. Table I shows the γ-transition energies, the relative transition intensities, the spin and parity (I^π) assignments in ^{143}La. The γ transition intensities are normalized to that of the 291.5-keV γ transition.

In a previous β-decay experiment in ^{143}La [15], the spin and parity (I^π) of the ground state were assigned as $7/2^+$ and the I^π's for the 29.9 and 291.5 keV levels were assigned as $3/2^+$ and $5/2^+$, respectively. So band (1) is built on the

*zhushj@mail.tsinghua.edu.cn

TABLE I. The γ-transition energies, the relative transition intensities, the assignments of spin and parity (I^π) values, and the $B(E1)/B(E2)$ branching ratios in ^{143}La.

E_γ (keV)	$I_i^\pi \rightarrow I_f^\pi$	I_γ (%)	$B(E1)/B(E2)$ (10^{-6} fm^{-2})
29.9	$3/2^+ \rightarrow 7/2^+$		
291.5	$5/2^+ \rightarrow 7/2^+$	100(2)	
261.5	$5/2^+ \rightarrow 3/2^+$	24(2)	
364.7		40(4)	
425.1	$(9/2^+) \rightarrow$	22(1)	
bands (1) & (2)			
498.3	$(9/2^+) \rightarrow 5/2^+$	56(2)	
535.6	$(11/2^-) \rightarrow (9/2^+)$	17(2)	
128.0	$(13/2^+) \rightarrow (11/2^-)$	0.97(23)	1.43(35)
663.6	$(13/2^+) \rightarrow (9/2^+)$	32(2)	
325.8	$(15/2^-) \rightarrow (13/2^+)$	15(2)	0.64(10)
453.8	$(15/2^-) \rightarrow (11/2^-)$	10(1)	
364.5	$(17/2^+) \rightarrow (15/2^-)$	1.8(3)	0.51(10)
690.3	$(17/2^+) \rightarrow (13/2^+)$	8.8(9)	
230.7	$(19/2^-) \rightarrow (17/2^+)$	1.7(3)	0.53(12)
595.2	$(19/2^-) \rightarrow (15/2^-)$	15(2)	
424.4	$(21/2^+) \rightarrow (19/2^-)$	1.6(3)	0.75(18)
655.1	$(21/2^+) \rightarrow (17/2^+)$	2.6(4)	
641.7	$(23/2^-) \rightarrow (19/2^-)$	8.1(8)	
614.1	$(27/2^-) \rightarrow (23/2^-)$	3.6(3)	
band (3)			
498.5		5.3(7)	
615.0		5.7(7)	
570.0	$\rightarrow (9/2^+)$	16(2)	
404.9	$\rightarrow (13/2^+)$	5.5(6)	

291.5 keV $5/2^+$ level. Based on the regular level spacings and the systematical comparison with the neighboring nuclei, we assigned band (1) as a positive parity band with $\Delta I = 2$ stretched $E2$ transitions inside the band, and the I^π's of other levels are assigned as $9/2^+$, $13/2^+$, $17/2^+$, and $21/2^+$, respectively. According to the internal conversion coefficient measurements and systematical comparison with the structures of neighboring isotopes ^{145,147}La [13,14], we establish band (2) as a negative parity band. This band should have $\Delta I = 2$ stretched $E2$ transitions inside the band also. We have measured a total internal conversion coefficient (α_T) of the low-energy crossing transition 128.0 keV from the 1453.4 keV level in band (1) to the 1325.4 keV level in band (2). This α_T is obtained by double gating on the 595.2 and 535.6 keV transitions. In this gate the difference in relative intensities of the 325.8 and 128.0 keV transitions is equal to the internal conversion electron intensity of the 128.0 keV transition. Because the partner nucleus ^{105}Nb has a 128.0 keV transition also [21], this measurement becomes a little complex. However, according to the intensity ratio of the 128.0 to 162.4 keV transitions in ^{105}Nb [21], we have eliminated the partner's contamination. The observed experimental α_T value is 0.16(5), and the theoretical value is 0.12 for an $E1$ transition and 0.53 for an $M1$ transition, respectively. So the 128.0-keV transition in ^{143}La is an $E1$ transition, but not an $M1$ one. According to the transition selection rule, the I^π of the 1325.4 keV level in band (2) should be assigned as $11/2^-$, and band (2) is a negative-parity band. The I^πs of other levels in this band are assigned as $15/2^-$, $19/2^-$, $23/2^-$, and $27/2^-$, respectively. Thus, bands (1) and (2) are firmly established with spins up to 21/2 and 27/2 $\hbar$, respectively.

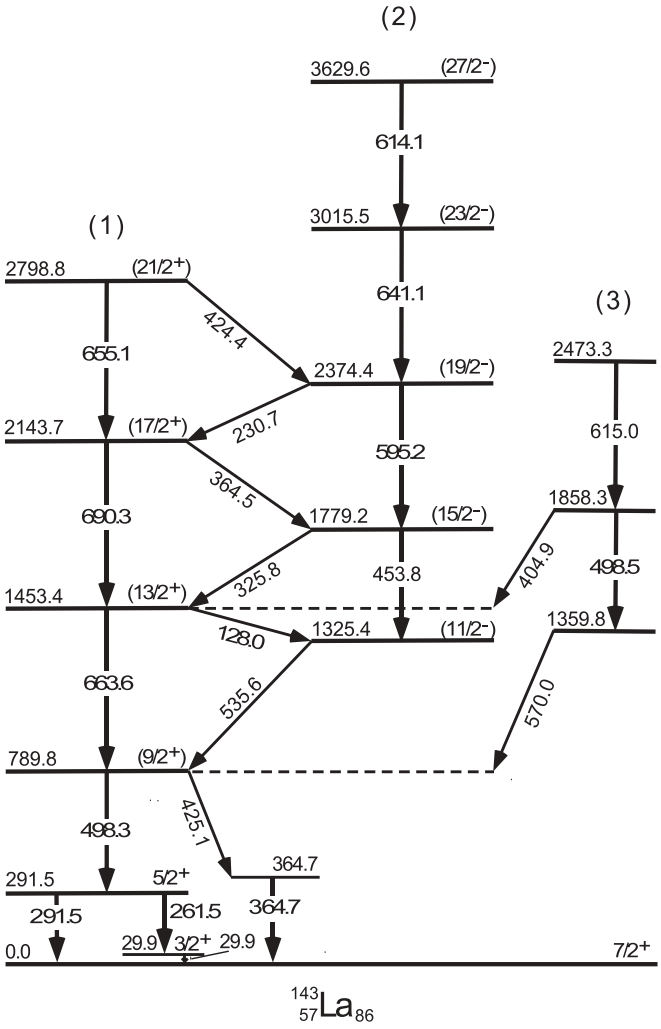

FIG. 1. Level scheme of ^{143}La.

III. DISCUSSION

From Fig. 1 one can see that a set of two bands (1) and (2) with the $\Delta I = 2E2$ transitions in each band along with the six intertwined $E1$ transitions, 535.6, 128.0, 325.8, 364.5, 230.7, and 424.4 keV between these two bands form a typical octupole collective-band structure. These levels indicate a reflection-asymmetric shape in ^{143}La similar to those observed in the neighboring Ba, La, Ce nuclei [4–14]. This octupole-band structure has a simplex quantum number $s = +i$ [1]. Figure 3 shows a systematic comparison of levels in the octupole-band structure in ^{143}La with those in the neighboring isotope ^{145}La [13] as well as in the $N = 86$ isotones ^{142}Ba [5] and ^{144}Ce [11]. We can see that the level structures in these octupole bands have similar character. However, the energies of the levels with the same spin in ^{143}La and ^{145}La

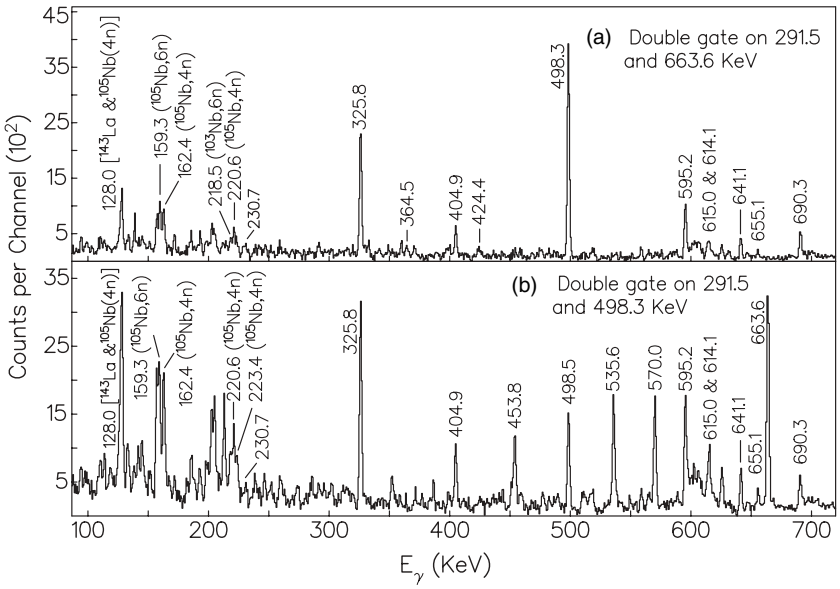

FIG. 2. The γ ray spectra of ^{143}La obtained from triple coincidences: (a) double gating on 291.5 and 663.6 keV transitions, and (b) double gating on 291.5 and 498.3 keV transitions.

are compared, those in ^{143}La are higher than those in ^{145}La. These differences may be related to the different quadrupole deformation in both isotopes. But the level spacings in ^{143}La are closer to those in the ^{142}Ba and ^{144}Ce isotones. This can be explained as the coupling of a single-particle or hole (proton) orbital in ^{143}La with the octupole-band core in the neighboring even-even ^{142}Ba or ^{144}Ce isotones, as discussed in Ref. [13].

A nucleus with octupole deformed bands decays through $E1$ and $E2$ transitions. The $B(E1)/B(E2)$ branching ratio is defined as

$$\frac{B(E1)}{B(E2)} = 0.771 \frac{I_\gamma(E1)E_\gamma(E2)^5}{I_\gamma(E2)E_\gamma(E1)^3}(10^{-6}\,\mathrm{fm}^{-2}), \qquad (1)$$

where the intensity (I_γ) and energy (E_γ) have been taken from the present work. The $B(E1)/B(E2)$ values in ^{143}La from our investigation are listed in Table I. The average value of the $B(E1)/B(E2)$ for the $s = +i$ band structure of ^{143}La is 0.77 (10^{-6} fm^{-2}). And the values observed for ^{142,144}Ba [5], ^{145,147}La [13], and ^{148}Ce [12] are 1.0, 0.70, 0.76, 0.58, and 0.82 (10^{-6} fm^{-2}), respectively. So the average value for ^{143}La is comparable with those in the neighboring nuclei. This similarity indicates that there are strong octupole correlations in ^{143}La also.

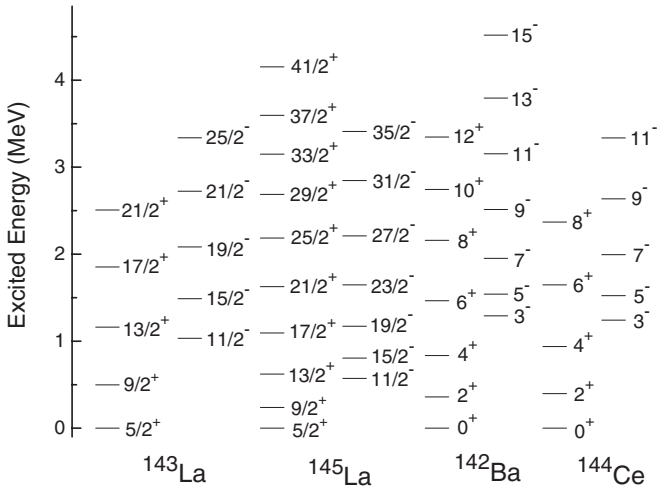

FIG. 3. Systematic comparison for the levels of $s = +i$ band structures in ^{143,145}La and $s = +1$ band structures in ^{142}Ba and ^{144}Ce.

Now we consider the octupole deformation stability with the spin variation of ^{143}La. The energy displacement δE and the rotational frequency ratio $\omega^-(\mathrm{I})/\omega^+(\mathrm{I})$ between the $\pi = +$ and $\pi = -$ bands are defined as [1,11]

$$\delta E(I) = E(I^-) - \frac{(I+1)E(I-1)^+ + IE(I+1)^+}{2I+1} \qquad (2)$$

and

$$\omega^-(I)/\omega^+(I) = 2\frac{E(I+1)^- - E(I-1)^-}{E(I+2)^+ - E(I-2)^+}. \qquad (3)$$

In the limit of the stable octupole deformation, $\delta E(I)$ should approach zero, and the rotational frequency ratio $\omega^-(I)/\omega^+(I)$ should be close to one. In the limit of aligned octupole vibration, the $\omega^-(I)/\omega^+(I)$ approaches the value $(2I-5)/(2I+1)$ [1]. Plots of δE and $\omega^-(I)/\omega^+(I)$ for the $s = +i$ band structure of ^{143}La, along with those of the $s = +1$ band structures of the $N = 86$ isotones ^{142}Ba [5] and ^{144}Ce [11] against spin I are shown in the Fig. 4. One can see that they have very similar behavior. As the spin I increases, δE approaches zero and the trend of $\omega^-(I)/\omega^+(I)$ is close to one. This shows that the octupole deformation becomes more stable as the spin increases in the $N = 86$ ^{142}Ba, ^{143}La, and ^{144}Ce isotones.

Plots of the kinetic moment of inertia (J_1) versus rotational frequency ($\hbar\omega$) for the $s = +i$ band structures of ^{143}La and ^{145}La [13] are shown in Fig. 5. One can see that the back-bendings (band crossings) for the $\pi = +$ and $\pi = -$ bands appear around 0.25–0.30 MeV in ^{145}La. As there is a lower fission yield in ^{143}La than in ^{145}La, we cannot observe higher-spin states in this experiment, and cannot see the full back-bendings in ^{143}La. However, from Fig. 5, we can see that the back-bendings begin around 0.30–0.35 MeV in ^{143}La. As the band crossings were explained by the alignment of

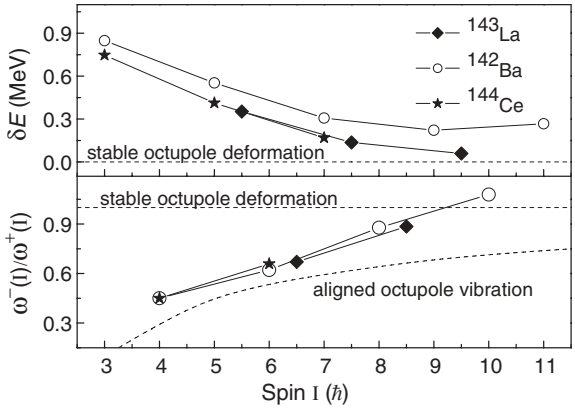

FIG. 4. Plots of δE and $\omega^-(I)/\omega^+(I)$ against spin I for the octupole band structures in ^{143}La, ^{142}Ba, and ^{144}Ce.

the two $i_{13/2}$ neutrons in ^{145}La [11], so the band crossings of ^{143}La may be caused by the alignment of a pair of neutrons also. This interpretation is reasonable because the crossing corresponding to two $h_{11/2}$ protons is blocked by the odd proton, as indicated in Ref. [13].

In order to further understand the octupole correlations, we have used the reflection-asymmetry shell model (RASM) [22,23] to calculate the level structure of ^{143}La. Here we briefly review the framework of the RASM. Considering a set of deformed BCS multiquasiparticle states $\{|\Phi_\kappa\rangle\}$, where κ identifies the quasiparticle configurations, we can construct a trial wave function

$$|\Psi\rangle = \sum_{IMK\kappa p} F^{Ip}_{MK\kappa} P^p P^I_{MK} |\Phi_\kappa\rangle, \tag{4}$$

where $\{P^p P^I_{MK}|\Phi_\kappa\rangle\}$ is a set of simultaneously angular-momentum- and parity-projected multiquasiparticle states which form the shell-model space. Here P^p and P^I_{MK} are the parity- and the angular-momentum-projection operators, respectively,

$$P^p = \tfrac{1}{2}(1 + p\hat{P}), \quad (p = \pm 1) \tag{5}$$

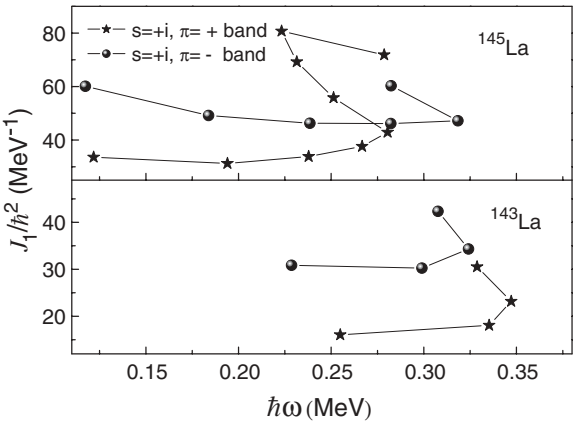

FIG. 5. Plots of moment of inertia (J_1) as a function of rotational frequency ($\hbar\omega$) in $s = +i$ band structures of ^{143,145}La.

and

$$P^I_{MK} = \frac{2I+1}{8\pi^2} \int d\Omega D^I_{MK}(\Omega) \hat{R}(\Omega). \tag{6}$$

The $F^{Ip}_{MK\kappa}$ is the coefficient to be determined by diagonalizing the shell-model Hamiltonian, namely solving the eigenvalue equation,

$$\sum_{K\kappa} \left\{ \langle \Phi_{\kappa'}| H P^p P^I_{K'K} |\Phi_\kappa\rangle - E^p_I \langle \Phi_{\kappa'}| P^p P^I_{K'K} |\Phi_\kappa\rangle \right\} F^{Ip}_{MK\kappa} = 0 \tag{7}$$

with the normalization condition,

$$\sum_{K'\kappa'K\kappa} F^{Ip*}_{MK'\kappa'} \langle \Phi_{\kappa'}| P^p P^I_{K'K} |\Phi_\kappa\rangle F^{Ip}_{MK\kappa} = 1. \tag{8}$$

It is seen that Eq. (7) is valid for any nuclear shape, while in the present study we consider the case of axial symmetry. The eigenvalues of H together with the wave functions can be calculated from Eq. (7). The intrinsic state $|\Phi_\kappa\rangle$ can be generated by doing a BCS transformation of the deformed single-particle states. In the present study, the single-particle states were calculated from a deformed Nilsson potential.

The Hamiltonian is written as

$$\hat{H} = \hat{H}_0 - \frac{1}{2} \sum_{\lambda=2}^{4} \chi_\lambda \sum_{\mu=-\lambda}^{\lambda} \hat{Q}^+_{\lambda\mu} \hat{Q}_{\lambda\mu} - G_M \hat{P}^+_{00} \hat{P}_{00} - G_Q \sum_{\mu=-2}^{2} \hat{P}^+_{2\mu} \hat{P}_{2\mu}, \tag{9}$$

where $\hat{H}_0$ is the spherical single-particle shell-model Hamiltonian, and the second term includes quadrupole ($\lambda = 2$), octupole ($\lambda = 3$), and hexadecapole ($\lambda = 4$) interactions, which lead to the quadrupole, octupole, and hexadecapole deformations, respectively; the third and fourth terms represent monopole and quadrupole pairing interactions, respectively. The coupling constants, χ_λ, can be determined to be consistent with the deformations [22]. Details about RASM were given in Ref. [22].

The Hamiltonian (9) is then diagonalized within the shell model space spanned by a selected set of the simultaneously parity- and angular-momentum-projected BCS multiquasiparticle states. As a primary application of RASM for odd-A nuclei, we only employed one proton quasiparticle state $a^\dagger_\pi \|0\rangle$, where π denotes the proton Nilsson quantum number which runs over properly selected low-lying quasiparticle states.

The Nilsson parameters κ and μ chosen in this calculation come from Refs. [23,24], and the monopole pairing strength constant G_M:

$$G_M = \left[g_1 \mp g_2 \left(\frac{N-Z}{A} \right) \right] \times A^{-1}, \tag{10}$$

where the minus (plus) sign represents neutron (proton). The parameters $g_1 = 18.0$ and $g_2 = 14.4$ are used [25]. The quadrupole pairing strength G_Q is assumed to be proportional to the monopole pairing strength: $G_Q = f_Q G_M$, and $f_Q = 0.16$ is chosen in this calculation. Considering the Ba core's and the neighboring nuclear deformation parameters [23,26],

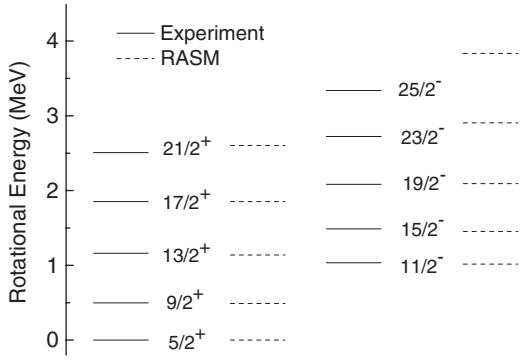

FIG. 6. The calculated energy levels of RASM and experimental energy levels for the $s = +i$ band structure in ^{143}La.

the quadrupole parameter $\epsilon_2 = 0.12$, the octupole $\epsilon_3 = 0.077$ and the hexadecapole $\epsilon_4 = -0.015$ are used. The calculated levels for the $s = +i$ band structures are compared with the experimental ones for ^{143}La in Fig. 6. They are in very good accord with each other through spin 19/2 $\hbar$. Above that, the theoretical values are larger than the experimental results. The reason may be that in the calculation we only consider single quasiparticle states right now. When the spin becomes higher, three quasiparticle states should be taken into account as also indicated by the backbend plots. The calculation indicates that ^{143}La indeed has a reflection-asymmetric shape. The I^{π}'s of the side band (3) are not clear.

IV. SUMMARY

In the present work, the high spin states in ^{143}La have been studied. Three collective bands have been established for the first time. An octupole-deformed band structure has been identified. Observed $B(E1)/B(E2)$ branching ratios indicate that the octupole correlations are strong in ^{143}La. The reflection-asymmetry shell model has been used to calculate the levels of the octupole bands, and basically the calculated results are in good agreement with the experimental ones up to the backbend.

ACKNOWLEDGMENTS

The work at Tsinghua University and the China Institute of Atomic Energy was supported by the National Natural Science Foundation of China under Grant Nos. 10575057 and 10647147, respectively. The work at Vanderbilt University, Lawrence Berkeley National Laboratory, was supported, respectively, by the U.S. Department of Energy under Grant and Contract Nos. DE-FG05-88ER40407 and DE-AC03-76SF00098.

[1] W. Nazarewicz and P. Olanders, Nucl. Phys. **A441**, 420 (1985).
[2] W. Nazarewicz, P. Olanders, I. Ragnarsson, J. Dudek, G. A. Leander, P. Moller, and E. Ruchowska, Nucl. Phys. **A429**, 269 (1984).
[3] G. A. Leander, W. Nazarewicz, P. Olanders, I. Ragnarsson, and J. Dudek, Phys. Lett. **B152**, 284 (1985).
[4] J. H. Hamilton, A. V. Ramayya, S. J. Zhu, G. M. Ter-Akopiam, Yu. Ts. Oganessian, J. D. Cole, J. O. Rasmusen, and M. A. Stoyer, Prog. Part. Nucl. Phys. **35**, 635 (1995).
[5] S. J. Zhu, Q. H. Lu, J. H. Hamilton, A. V. Ramayya, L. K. Peker, M. G. Wang, W. C. Ma, B. R. S. Babu, T. N. Ginter, J. Kormicki, D. Shi, J. K. Deng, W. Nazarewicz, J. O. Rasmussen, M. A. Stoyer, S. Y. Chu, K. E. Gregorich, M. F. Mohar, S. Asztalos, S. G. Prussin, J. D. Cole, R. Aryaeinejad, Y. K. Dardenne, M. Drigert, K. J. Moody, R. W. Loughed, J. F. Wild, N. R. Johnson, I. Y. Lee, F. K. McGowan, G. M. Ter-Akopian, and Yu. Ts. Oganessian, Phys. Lett. **B357**, 273 (1995).
[6] Y. X. Luo, J. O. Rasmussen, J. H. Hamilton, A. V. Ramayya, J. K. Hwang, C. J. Beyer, S. J. Zhu, J. Kormicki, X. Q. Zhang, E. F. Jones, P. M. Gore, T. N. Ginter, K. E. Gregorich, I. Y. Lee, A. O. Macchiavelli, P. Zielinski, C. M. Folden III, P. Fallon, G. M. Ter-Akopian, Yu. Ts. Oganessian, A. V. Daniel, M. A. Stoyer, J. D. Cole, R. Donangelo, S. C. Wu, and S. J. Asztalos, Phys. Rev. C **66**, 014305 (2002).
[7] M. A. Jones, W. Urban, J. L. Durell, M. Leddy, W. R. Phillips, A. G. Smith, B. J. Varley, I. Ahmad, L. R. Morss, M. Bentaleb, E. Lubkiewicz, and N. Schulz, Nucl. Phys. **A605**, 133 (1996).
[8] S. J. Zhu, J. H. Hamilton, A. V. Ramayya, E. F. Jones, J. K. Hwang, M. G. Wang, X. Q. Zhang, P. M. Gore, L. K. Peker, G. Drafta, B. R. S. Babu, W. C. Ma, G. L. Long, L. Y. Zhu, C. Y. Gan, L. M. Yang, M. Sakhaee, M. Li, J. K. Deng, T. N. Ginter, C. J. Beyer, J. Kormicki, J. D. Cole, R. Aryaeinejad, M. W. Drigert, J. O. Rasmussen, S. Asztalos, I. Y. Lee, A. O. Macchiavelli, S. Y. Chu, K. E. Gregorich, M. F. Mohar, G. M. Ter-Akopian, A. V. Daniel, Yu. Ts. Oganessian, R. Donangelo, M. A. Stoyer, R. W. Lougheed, K. J. Moody, J. F. Wild, S. G. Prussin, J. Kliman, and H. C. Griffin, Phys. Rev. C **60**, 051304(R) (1999).
[9] W. R. Phillips, I. Ahmad, H. Emling, R. Holzmann, R. V. F. Janssens, T. L. Khoo, and M. W. Drigert, Phys. Rev. Lett. **57**, 3257 (1986).
[10] W. R. Phillips, R. V. F. Janssens, I. Ahmad, H. Emling, R. Holzmann, T. L. Khoo, and M. W. Drigert, Phys. Lett. **B212**, 402 (1988).
[11] L. Y. Zhu, S. J. Zhu, M. Li, J. H. Hamilton, A. V. Ramayya, B. R. S. Babu, W. C. Ma, J. O. Rasmussen, M. A. Stoyer, and I. Y. Lee, High Energy Phys. Nucl. Phys. **22**, 885 (1998) (in Chinese).
[12] Y. J. Chen, S. J. Zhu, J. H. Hamilton, A. V. Ramayya, J. K. Hwang, M. Sakhaee, Y. X. Luo, J. O. Rasmussen, K. Li, I. Y. Lee, X. L. Che, H. B. Ding, and M. L. Li, Phys. Rev. C **73**, 054316 (2006).
[13] S. J. Zhu, J. H. Hamilton, A. V. Ramayya, M. G. Wang, J. K. Hwang, E. F. Jones, L. K. Peker, B. R. S. Babu, G. Drafta, W. C. Ma, G. L. Long, L. Y. Zhu, M. Li, C. Y. Gan, T. N. Ginter, J. Kormicki, J. K. Deng, D. T. Shi, W. E. Collins, J. D. Cole, R. Aryaneinejad, M. W. Drigert, J. O. Rasmussen, R. Donangelo, J. Gilat, S. Asztalos, I. Y. Lee, A. O. Macchiavelli, S. Y. Chu, K. E. Gregorich, M. F. Mohar, M. A. Stoyer, R. W. Lougheed, K. J. Moody, J. F. Wild, S. G. Prussin, G. M. Ter-Akopian, A. V. Daniel, and Yu. Ts. Oganessian, Phys. Rev. C **59**, 1316 (1999).
[14] W. Urban, W. R. Phillips, J. L. Durell, M. A. Jones, M. Leddy, C. J. Pearson, A. G. Smith, B. J. Varley, I. Ahmad, L. R. Morss,

M. Bentaleb, E. Lubkiewicz, and N. Schulz, Phys. Rev. C **54**, 945 (1996).
[15] S. H. Faller, J. D. Robertson, E. M. Baum, C. Chung, C. A. Stone, and W. B. Walters, Phys. Rev. C **38**, 307 (1988).
[16] J. C. Pacer, J. C. Hill, D. G. Shirk, and W. L. Talbert, Jr., Phys. Rev. C **17**, 710 (1978).
[17] F. Schussler, J. Blachost, E. Monnand, B. Fogelberg, S. H. Feenstra, J. V. Kinken, G. Jung, and K. D. Wunsch, Z. Phys. A **290**, 359 (1979).
[18] I. Y. Lee, Nucl. Phys. **A520**, 641c (1990).
[19] D. C. Radford, Nucl. Instrum. Methods Phys. Res. A **361**, 297 (1995).
[20] J. K. Hwang, A. V. Ramayya, J. Gilat, J. H. Hamilton, L. K. Peker, J. O. Rasmussen, J. Kormicki, T. N. Ginter, B. R. S. Babu, C. J. Beyer, E. F. Jones, R. Donangelo, S. J. Zhu, H. C. Griffin, G. M. Ter Akopian, Yu. Ts. Oganessian, A. V. Daniel, W. C. Ma, P. G. Varmette, J. D. Cole, R. Aryaeinejad, M. W. Drigert, and M. A. Stoyer, Phys. Rev. C **58**, 3252 (1998).
[21] Y. X. Luo, J. O. Rasmussen, I. Stefanescu, A. Gelberg, J. H. Hamilton, A. V. Ramayya, J. K. Hwang, S. J. Zhu, P. M. Gore, D. Fong, E. F. Jones, S. C. Wu, I. Y. Lee, T. N. Ginter, W. C. Ma, G. M. Ter-Akopian, A. V. Daniel, M. A. Stoyer, and R. Donangelo, J. Phys. G: Nucl. Part. Phys. **31**, 1303 (2005).
[22] Y. S. Chen and Z. C. Gao, Phys. Rev. C **63**, 014314 (2000).
[23] Y. J. Chen, Y. S. Chen, S. J. Zhu, Z. C. Gao, and Y. Tu, Chin. Phys. Lett. **22**, 1362 (2005).
[24] J. Y. Zhang, N. Xu, D. B. Fossan, Y. Liang, R. Ma, and E. S. Paul, Phys. Rev. C **39**, 714 (1989).
[25] Y. Sun and M. Guidry, Phys. Rev. C **52**, R2844 (1995).
[26] P. A. Bulter and W. Nazarwicz, Nucl. Phys. **A533**, 249 (1991).